Lipid-induced insulin resistance mediated by the proinflammatory receptor TLR4 requires saturated fatty acid–induced ceramide biosynthesis in mice

William L. Holland,[1] Benjamin T. Bikman,[2] Li-Ping Wang,[3] Guan Yuguang,[2] Katherine M. Sargent,[4] Sarada Bulchand,[2] Trina A. Knotts,[5] Guanghou Shui,[6] Deborah J. Clegg,[1] Markus R. Wenk,[6] Michael J. Pagliassotti,[7] Philipp E. Scherer,[1] and Scott A. Summers[2,3,4]

[1]Department of Internal Medicine, University of Texas Southwestern Medical Center, Dallas, Texas, USA. [2]Program in Cardiovascular and Metabolic Diseases, Duke-National University of Singapore Graduate Medical School, Singapore. [3]Sarah W. Stedman Nutrition and Metabolism Center, Duke University Medical Center, Durham, North Carolina, USA. [4]Division of Endocrinology, Metabolism, and Diabetes, Department of Internal Medicine, University of Utah, Salt Lake City, Utah, USA. [5]United States Department of Agriculture, Agricultural Research Service Western Human Nutrition Research Center, Davis, California, USA. [6]Department of Biochemistry, National University of Singapore, Singapore. [7]Department of Nutrition, Colorado State University, Fort Collins, Colorado, USA.

Obesity is associated with an enhanced inflammatory response that exacerbates insulin resistance and contributes to diabetes, atherosclerosis, and cardiovascular disease. One mechanism accounting for the increased inflammation associated with obesity is activation of the innate immune signaling pathway triggered by TLR4 recognition of saturated fatty acids, an event that is essential for lipid-induced insulin resistance. Using in vitro and in vivo systems to model lipid induction of TLR4-dependent inflammatory events in rodents, we show here that TLR4 is an upstream signaling component required for saturated fatty acid–induced ceramide biosynthesis. This increase in ceramide production was associated with the upregulation of genes driving ceramide biosynthesis, an event dependent of the activity of the proinflammatory kinase IKKβ. Importantly, increased ceramide production was not required for TLR4-dependent induction of inflammatory cytokines, but it was essential for TLR4-dependent insulin resistance. These findings suggest that sphingolipids such as ceramide might be key components of the signaling networks that link lipid-induced inflammatory pathways to the antagonism of insulin action that contributes to diabetes.

Introduction

Insulin promotes postprandial absorption and storage of glucose, with skeletal muscle being the major site of carbohydrate deposition. When muscle fibers are simultaneously exposed to exogenous fatty acids or lipoprotein-bound triglycerides they become insulin resistant, a metabolic state which predisposes individuals to cardiovascular disease and diabetes (1, 2). Saturated fatty acids (SFAs), but not unsaturated fatty acids, induce the formation of sphingolipids (i.e., ceramide and glucosylceramides), which are potent antagonists of insulin action (3). The implementation of pharmacological or genetic strategies to inhibit ceramide biosynthesis in rodents dramatically improves insulin sensitivity and prevents many of the deleterious metabolic abnormalities (e.g., atherosclerosis, cardiomyopathy, diabetes) associated with insulin resistance (3–10).

SFAs are agonists for TLR4 (11–15), a pattern-recognition receptor that is essential for mounting inflammatory responses associated with innate immunity. Thus, TLR4 emerged as a candidate intermediary linking obesity and dyslipidemia to enhanced inflammatory cytokine production. A study by Shi et al. demonstrated that TLR4 is essential for acute, lipid-induced insulin resistance (15). Moreover, studies in animals fed high-fat diets have revealed that TLR4 deletion improves peripheral insulin sensitivity (16–19). Because both ceramide biosynthesis and TLR4 activation are highly selective for SFAs, we hypothesized that TLR4 and ceramide might lie in a linear signaling pathway linking exogenous fats to the disruption of insulin action. Our present study demonstrates that the accumulation of ceramide in skeletal muscle and liver is highly dependent upon inflammatory events controlled by TLR4.

Results

Infusion of lard oil, but not soy oil, induces inflammation and insulin resistance in rats. Experimental infusion of triglyceride-heparin emulsions into the bloodstream of rodents and humans has become a common experimental strategy for assessing the mechanisms by which lipids alter insulin secretion and action. In 1997, the McGarry group demonstrated that the relative composition of the infusate is a critical determinant of experimental design, as soy-based cocktails enriched in unsaturated fats inhibited insulin secretion, while a lard-infusate containing a higher percentage of saturated fats had the opposite effect (20). Using an experimental protocol comparable to that utilized by the McGarry group, we evaluated the effects of saturated vs. unsaturated fats on insulin-stimulated glucose disposal. As compared with a 2.5% glycerol infusate, delivery of either a lard- or soy-based cocktail markedly inhibited rates of insulin-stimulated glucose disposal (Figure 1A) and increased levels of diacylglycerol (DAG) in soleus muscle (Figure 1C). However, only lard oil increased muscle ceramide levels (Figure 1B).

Authorship note: William L. Holland and Benjamin T. Bikman are co–first authors.

Conflict of interest: Scott A. Summers acknowledges having financial relationships with Hoffman-La Roche and AstraZeneca.

Citation for this article: *J Clin Invest.* 2011;121(5):1858–1870. doi:10.1172/JCI43378.

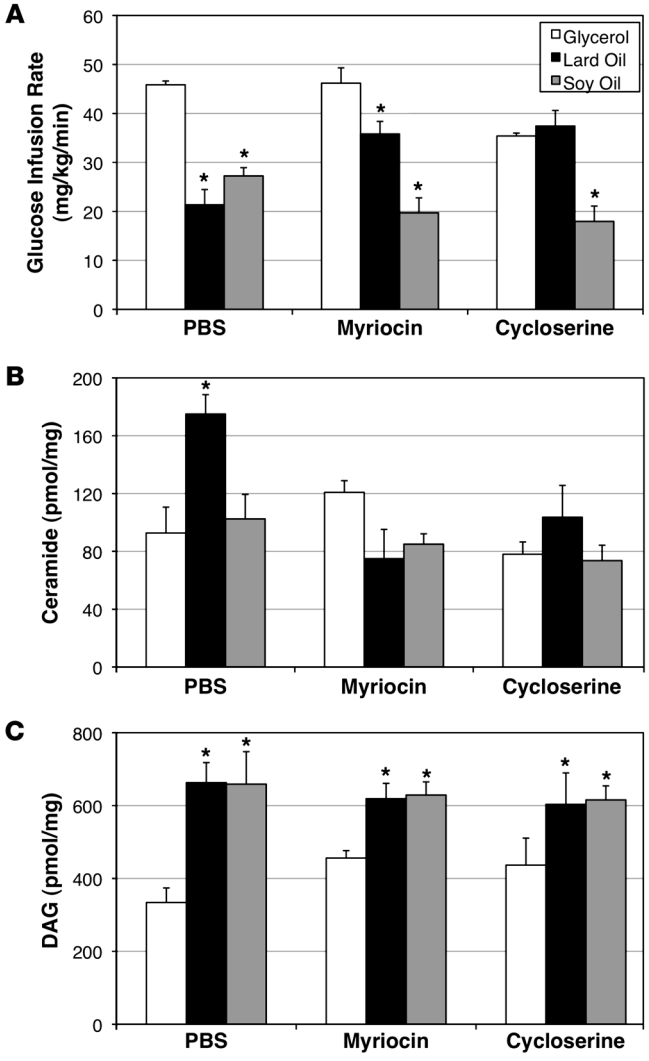

Figure 1
Lard oil infusion inhibits insulin-stimulated glucose uptake in a ceramide-dependent manner. (**A**) Whole body glucose disposal was assessed by hyperinsulin-euglycemic clamp during infusion with lard oil (black bars), soy oil (white bars), or glycerol (gray bars) following treatment with inhibitors myriocin, cycloserine, or PBS. (**B** and **C**) Ceramide (**B**) and DAG (**C**) content was enzymatically determined using the DAG-kinase assay from soleus muscle following 6 hours of lipid infusion. Values are expressed as mean ± SEM ($n = 8$). *$P < 0.05$ for lard or soy oil versus glycerol within a given treatment.

To determine the quantitative importance of ceramides as modulators of lard-induced insulin resistance, we treated the animals with inhibitors (i.e., myriocin or cycloserine) of serine palmitoyltransferase (SPT), the enzyme responsible for the first committed step toward ceramide biosynthesis. As shown in Figure 1, both myriocin and cycloserine prevented lard induction of insulin resistance (Figure 1A) and ceramide accumulation (Figure 1B) but had no effect on the soy-induced insulin resistance. Neither compound reduced DAG levels (Figure 1C). Collectively, these data indicate that ceramide synthesis is essential for lard-induced insulin resistance but is dispensable for that caused by soy oil. These data confirm that different fatty acids induce insulin resistance via distinct mechanisms that can be discerned by their reliance on ceramide.

We predicted that the lard oil, because of its elevated SFA content, would induce a more pronounced inflammatory response than could be achieved using the soy-based infusate. Consistent with this hypothesis, lard oil infusion had a striking effect on circulating IL-6 and TNF-α levels, which increased several-fold in the lard-infused rats (Figure 2, A and B, respectively). Molecular analysis of the lard oil infusate indicated that it was free of endotoxin (data not shown). Co-infusing the inhibitors of ceramide biosynthesis, which normalized insulin sensitivity, did not reduce circulating cytokine levels.

TLR4 deletion prevents SFA-induced cytokine release and insulin resistance. To confirm that the inflammatory response caused by lard oil infusion was mediated by TLR4-dependent signaling pathways, we measured cytokine levels in mice expressing a defective TLR4 ($Tlr4^{lps\text{-}d}$). As we saw in the rats, lard oil infusion markedly increased serum cytokine levels in WT ($Tlr4^{+/+}$) mice (Figure 2C). However, mice lacking functional TLR4 ($Tlr4^{lps\text{-}d}$) showed a diminution in circulating TNF-α and IL-6 following lipid infusion (Figure 2C). To test the relevance of the TLR4 pathway on insulin sensitivity in this experimental model, we performed hyperinsulinemic-euglycemic clamps on the TLR4-knockout animals during the final 1.5 hours of lipid infusion. As shown in Figure 2D, $Tlr4^{lps\text{-}d}$ mice were protected from insulin resistance caused by lard oil infusion but were susceptible to insulin resistance caused by soy oil (Figure 2D). Mice lacking MyD88 (an adapter protein requisite for TLR signaling), but not those lacking TLR2, were also protected from lard-induced insulin resistance (Figure 2E).

TLR4 deletion selectively blocks LPS inhibition of glucose uptake in skeletal muscle. The data presented thus far indicate that both TLR4 and ceramide are required for lard oil–induced insulin resistance, but they are dispensable for that caused by soy oil. Thus, TLR4 and ceramide reside in either linear or parallel signaling pathways linking excess saturated lipids to the antagonism of insulin action. To explore relationships between inflammation and ceramide, we turned to an isolated muscle system, which allows us to evaluate tissue-autonomous effects of individual lipids on muscle insulin sensitivity. Using this system, we have previously shown that palmitate antagonizes insulin-stimulated glucose uptake via a ceramide-dependent mechanism (3). The data described below reveal that the TLR4 agonist LPS also antagonizes insulin-stimulated 2-deoxyglucose (2-DOG) uptake via ceramide. As shown in Figure 3A, LPS inhibited 2-DOG uptake in soleus muscles obtained from $Tlr4^{+/+}$ mice, but had no effect in muscles isolated from the $Tlr4^{lps\text{-}d}$ animals (Figure 3A). LPS additionally stimulated the production of ceramide, as intramyocellular levels of the lipid rose several-fold during a 6-hour LPS treatment (Figure 3B). To test the importance of this ceramide in LPS responses, we used 2 separate experimental approaches to block rates of de novo ceramide synthesis. First, we pretreated with the aforementioned inhibitor of SPT, myriocin. Second, we utilized muscles obtained from mice heterozygous for dihydroceramide desaturase (Des1), which we previously demonstrated are compromised in their ability to produce ceramide (3). As shown in Figure 3A, both of these experimental approaches negated LPS-induced insulin resistance.

We additionally chose to investigate the relationships between palmitate, TLR4, and ceramide using the isolated muscle system, where we had previously demonstrated that the SFA antagonized glucose transport by inducing ceramide synthesis (3). As shown in Figure 3, C and D, $Tlr4^{lps\text{-}d}$ mice were resistant to palmitate, as it failed to antagonize insulin-stimulated glucose transport

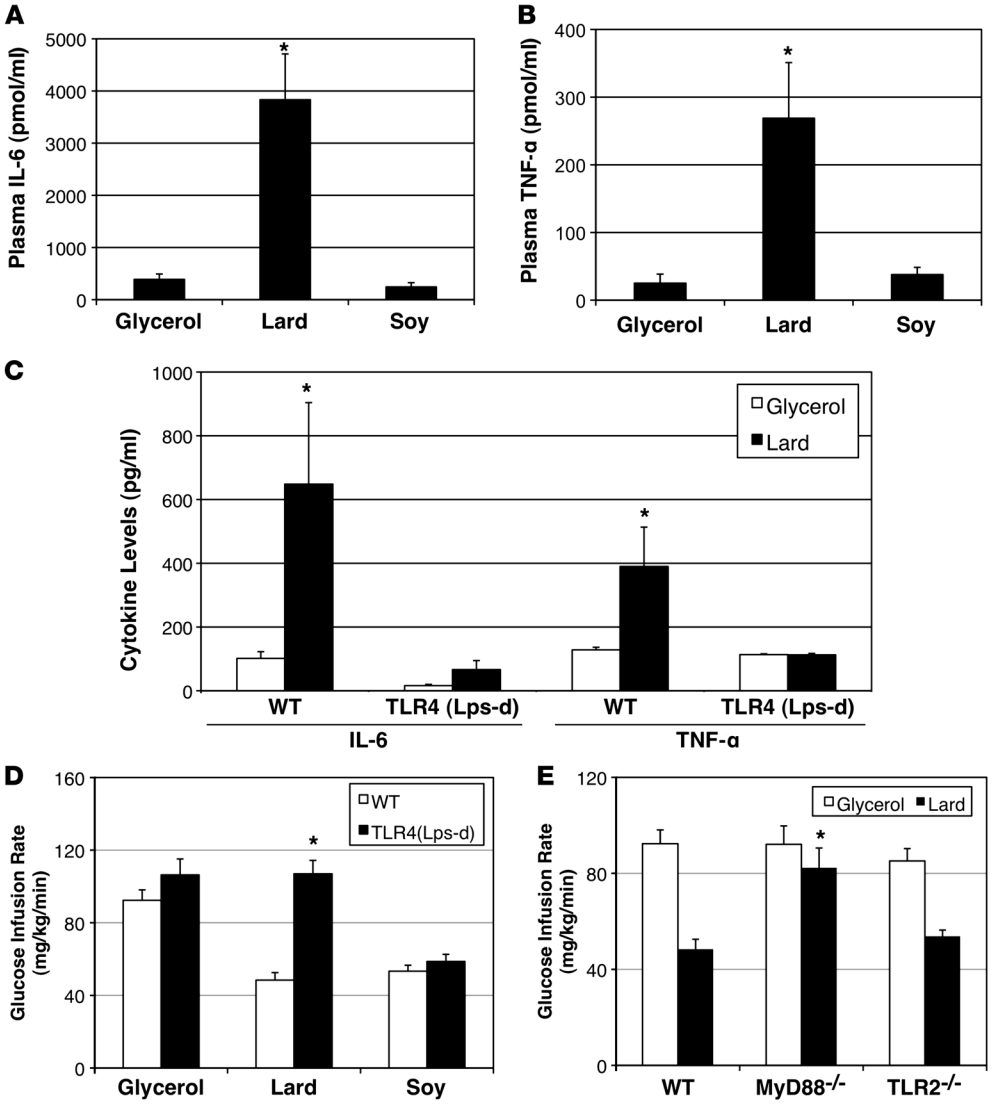

Figure 2
Lard oil infusion increases circulating inflammatory cytokine concentrations and impairs insulin-stimulated glucose disposal in a TLR4-dependent manner. (**A** and **B**) Plasma concentrations of IL-6 (**A**) and TNF-α (**B**) were determined using ELISA following a 6-hour infusion of glycerol, lard oil, or soy oil emulsions into male Sprague-Dawley rats. (**C**) Serum concentrations of IL-6 and TNF-α were measured using ELISA after 6 hours of glycerol or lard oil infusion into WT mice or TLR4-defective mice. (**D**) Whole body glucose disposal was assessed by hyperinsulinemic-euglycemic clamp initiated after 4.5 hours of glycerol, lard oil, or soy oil infusion into WT mice (white bars) or TLR4-defective mice (black bars). (**E**) Whole body glucose disposal was assessed by hyperinsulinemic-euglycemic clamp initiated after 4.5 hours of glycerol (white bars) or lard oil (black bars) infusion into WT mice, MyD88-null mice, or TLR2-null mice. Values are expressed as mean ± SEM (n = 6). *P < 0.05 for treatment versus glycerol control.

or induce ceramide accrual. In contrast, palmitate promoted ceramide accumulation and inhibited glucose uptake in muscles from WT or *Tlr2*$^{-/-}$ rodents. To evaluate the specificity of this response, we evaluated whether TLR4 inactivation altered rates of glycerolipid (i.e., DAG) synthesis or lipid oxidation. As shown in Figure 3E, palmitate induced DAG accumulation comparably in muscles from WT, *Tlr2*$^{-/-}$, and *Tlr4*$^{lps\text{-}d}$ mice. Moreover, the *Tlr4*$^{lps\text{-}d}$ mice demonstrated an enhanced rate of palmitate oxidation (Figure 3F). These data strongly indicate that ceramide or a ceramide metabolite, and not DAG or products generated during lipid oxidation, are key intermediates linking both palmitate and TLR4 to the antagonism of insulin action.

One of the cytokines induced by SFAs and TLR4 is TNF-α, which has long been implicated in insulin resistance and which induces ceramide by activating sphingomyelinase or by promoting its de novo ceramide synthesis. TNF-α was unable to induce insulin resistance, either in control muscle strips (data not shown) or in those obtained from the *Tlr4*$^{lps\text{-}d}$ mice (Supplemental Figure 1A; supplemental material available online with this article; doi:10.1172/JCI43378DS1). However, TNF-α was capable of recapitulating the TLR4 effect, as its re-addition in concert with palmitate antagonized glucose uptake in *Tlr4*$^{lps\text{-}d}$ muscles (Supplemental Figure 1A). Mice lacking TNF receptors were not protected from lard-induced insulin resistance (Supplemental Figure 1B). Thus, while TNF-α was sufficient to recapitulate the insulin-desensitizing role of LPS in muscles from *Tlr4*$^{lps\text{-}d}$ mice, it was not necessary.

Tlr4$^{lps\text{-}d}$ *mice fail to accrue ceramides with hyperlipidemia*. Rates of ceramide synthesis have long been thought to be controlled primarily by the availability of palmitoyl-CoA, which is a substrate for SPT and is required for formation of the sphingosine backbone. The data presented in this study suggest a different mechanism through which excessive fat promotes ceramide accrual. Specifically, these results indicate that lipid-activation of TLR4 leads to an upregulation of sphingolipid synthesis. To confirm this mechanism in vivo, we evaluated ceramide levels in the lard-infused mice (Figure 4). Lard oil infusion increased ceramide levels in both liver (Figure 4A) and muscle (Figure 4B) in *Tlr4*$^{+/+}$ mice but failed to induce it in either tissue in the *Tlr4*$^{lps\text{-}d}$ mice. Lard oil infusion did increase DAG levels in both tissues (Figure 4D), indicating that TLR4 receptor ablation specifically impairs sphingolipid synthesis

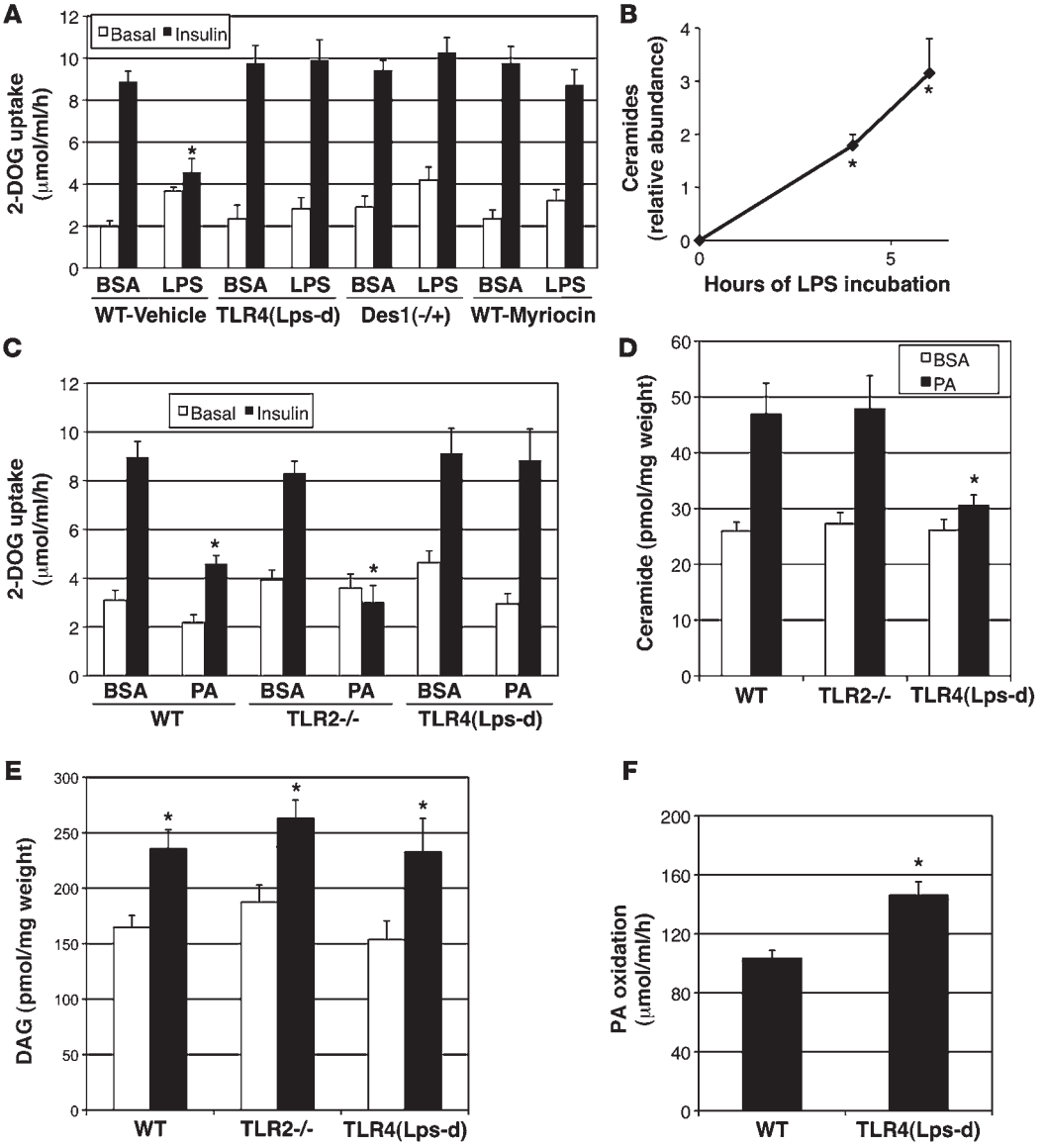

Figure 3

LPS and palmitate (PA) impair insulin-stimulated glucose uptake in isolated muscles via sphingolipid- and TLR4-dependent mechanisms. (**A** and **B**) Bisected soleus muscle strips from male Sprague Dawley rats were incubated for 6 hours in the presence or absence of LPS (100 ng/ml). (**A**) 2-DOG uptake was quantified under basal (white) or insulin-stimulated (black; 300 μU/ml) conditions following treatment with LPS or BSA control for 6 hours. *$P < 0.05$ compared with BSA conditions. (**B**) Ceramide was enzymatically quantified after 0, 4, or 6 hours of LPS treatment. *$P < 0.05$ for PA at 4 and 6 hours versus 0 hours. (**C**) Whole soleus muscles from WT, TLR2-null, or TLR4-defective mice were incubated for 6 hours in PA (1 mM) prior to measuring hexose uptake under basal (white bars) or insulin-stimulated (300 μU/ml; black bars) conditions. *$P < 0.05$ compared with BSA conditions. (**D** and **E**) After duplicate 6-hour treatments, ceramide (**D**) and DAG (**E**) were enzymatically quantified from lipid extracts of whole soleus muscle ($n = 6$) following treatment with BSA (white bars) and PA (black bars). *$P < 0.05$ for PA versus BSA. (**F**) The rate of PA oxidation was quantified ex vivo from whole soleus muscle of WT and TLR4-defective mice. *$P < 0.05$ for *Tlr4*$^{lps\text{-}d}$ compared with WT. Values are expressed as mean ± SEM ($n = 6$–8).

in peripheral tissue without affecting lipid uptake or bulk storage. To assess insulin sensitivity, we performed hyperinsulinemic-euglycemic clamps. Coincident with the reduction in ceramide levels, the *Tlr4*$^{lps\text{-}d}$ mice demonstrated a substantial improvement in muscle and liver insulin sensitivity, as evidenced by a higher rate of glucose infusion to maintain euglycemia, increased whole body glucose disposal, and reduced hepatic glucose output (Figure 4, E–G).

The hypothalamus has an emerging role in the regulation of hepatic glucose efflux, and SFAs have been shown to promote central leptin and insulin resistance associated with reduced activation of the anabolic enzyme Akt/protein kinase B (21–24). Lipid infusion significantly increased hypothalamic ceramide content of WT mice (Figure 4C). In contrast, no change in ceramides was detected in the hypothalamus of *Tlr4*$^{lps\text{-}d}$ mice

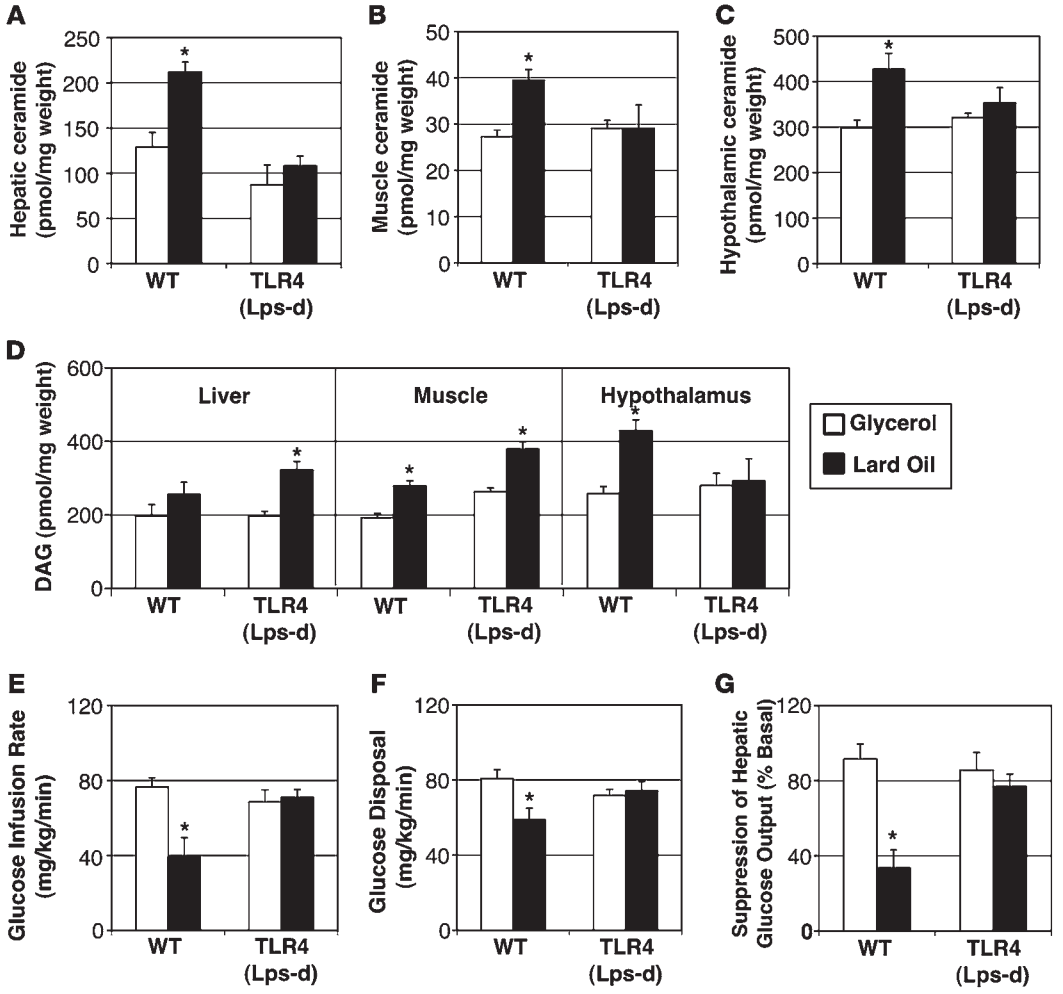

Figure 4

TLR4 signaling is essential for lipid-induced ceramide accumulation. Following 6 hours of intravenous infusion of glycerol (white bars) or lard oil (black bars), ceramides (**A**–**C**) were enzymatically determined from liver (**A**), muscle (**B**), or hypothalamus (**C**). (**D**) DAG was simultaneously measured in the same tissues. (**E**–**G**) Glucose kinetics were determined during hyperinsulinemic-euglycemic clamps (4 mU/kg/min insulin). (**E**) The glucose infusion rate required to maintain euglycemia was recorded. (**F**) Glucose disposal was calculated from ^{3}H-glucose turnover. (**G**) Hepatic glucose production was calculated during basal and insulin-stimulated conditions and presented as percent suppression by insulin (n = 5–6). *P < 0.05 for lard oil compared with glycerol.

following lard oil infusion (Figure 4D). Contrary to effects seen in peripheral tissues, *Tlr4*$^{lps\text{-}d}$ mice also fail to accumulate DAG in the hypothalamus (Figure 4D).

TLR4 agonists stimulate ceramide synthesis in both myotubes and macrophages. The studies in isolated muscle fibers revealed that the SFA-TLR4 pathway leading to sphingolipid synthesis and insulin resistance could be recapitulated in a tissue-autonomous system. Whole skeletal muscle consists of a variety of cell types in addition to myocytes such as macrophages and leukocytes. Though macrophages are known to contain TLR4, recent studies suggest they are located in myotubes and are upregulated in muscle cultured from obese and insulin-resistant humans (25). Thus, we sought to determine whether the effects of TLR4 stimulation on skeletal muscle sphingolipid metabolism and insulin sensitivity resulted from effects in myotubes, or instead resulted from effects in resident macrophages. We conducted an extensive lipidomic analysis of both C_2C_{12} myocytes and RAW264.7 macrophages treated with palmitate or LPS. Of all the lipids tested, only ceramide (in both myotubes and macrophages) and glucosylceramide (only in macrophages) increased in response to both LPS and palmitate (Figure 5). Other sphingolipids (i.e., GM3 ganglioside and sphingomyelin) levels were unchanged (data not shown). Glycerolipids (i.e., DAG and TAG) increased with palmitate in both cell types but were unaffected by LPS (Figure 5).

We next tested whether the ceramide generated within these cell types via the TLR4 agonists elicit biological responses, including impairment of insulin signaling (in myotubes) and cytokine generation (in macrophages). We previously demonstrated that relatively small increases in cellular ceramide levels, within the range observed in the lipid infusion and isolated muscle experiments described herein, are sufficient to inhibit insulin stimulation of the serine/threonine kinase Akt/PKB (26). Moreover, our prior studies have confirmed that this is the primary mechanism through which ceramides inhibit glucose transport (27). We thus tested whether LPS was capable of

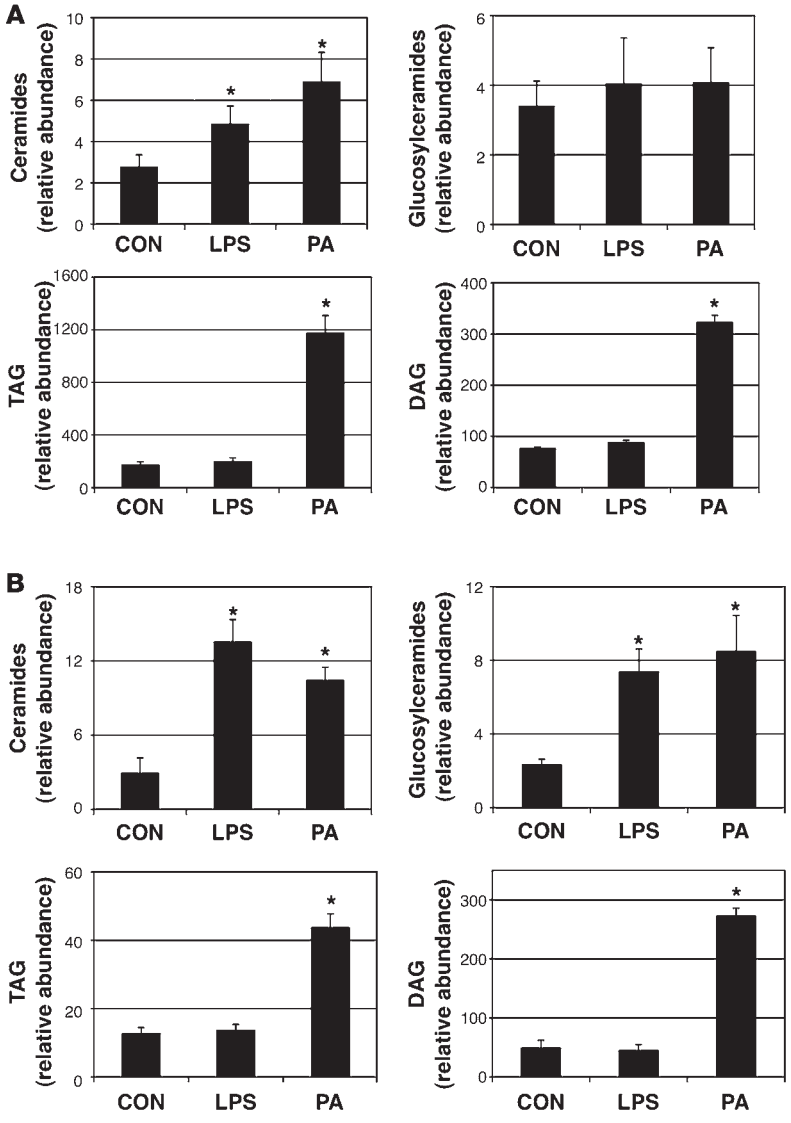

Figure 5
LPS and PA elicit an increase in sphingolipid synthesis. Lipids were determined in murine C_2C_{12} myotubes (**A**) and RAW264.7 macrophages (**B**) challenged with PA and LPS. LC-MS was performed to determine ceramides, glucosylceramides, TAG, and DAG in cells treated with LPS (1 μg/ml for myotubes; 100 ng/ml for macrophages) and PA (0.75 mM for myotubes; 0.45 mM for macrophages) for 16 hours. Values are expressed as mean ± SEM (n = 4). *P < 0.05 for treatment compared with BSA control (CON).

inhibiting Akt/PKB in a cell-autonomous system. As shown in Figure 6A, both LPS and palmitate were effective at inhibiting insulin-stimulated activation of Akt/PKB. Moreover, they inhibited insulin-stimulated phosphorylation of glycogen synthase kinase 3β, an Akt/PKB substrate. The inclusion of linoleate (LA) into either palmitate or LPS treatment had little effect on signaling or ceramides (Supplemental Figure 2). In macrophages, both LPS and palmitate, but not the unsaturated fatty acid LA, increased mRNA levels of TNF (Figure 6B). This transcriptional effect of palmitate on TNF-α was unaffected by myriocin or the ceramide synthase (CerS) inhibitor fumonisin B1, confirming that the effect is ceramide independent.

IKKβ is essential for TLR4-mediated insulin resistance and ceramide synthesis. A critical factor in many TLR4 responses is the transcription factor NF-κB, which translocates to the nucleus upon TLR4 activation and drives the synthesis of stress-induced cytokines. A family of IκB kinases (IKK) activates NF-κB signaling by phosphorylating inhibitor of NF-κB (IκBα), a protein that sequesters NF-κB in the cytosol. Once phosphorylated, IκBα releases NF-κB, and is itself degraded by the proteasome. NF-κB then translocates into the nucleus and upregulates genes associated with inflammation. IKKβ is well known for disruption of insulin responsiveness (28) and thus emerged as a likely modulator of insulin sensitivity and ceramide synthesis in this model system. To test the role of IKKβ in mediating TLR4-induced insulin resistance and ceramide accrual, stable C_2C_{12} lines expressing WT (IKK-WT) or dominant-negative (kinase-dead IKKβ [IKK-KD]; K44M) isoform were generated. Overexpression of IKK-KD, but not IKK-WT, prevented LPS-induced degradation of IκBα (Figure 7A). Lipidomic analysis revealed that inhibition of IKKβ signaling dramatically and selectively reduced levels of ceramides (Figure 7B), preventing ceramide induction by either palmitate or LPS. The cells expressing the IKK-KD were also resistant to palmitate- and LPS-inhibition of insulin signaling to Akt/PKB (Figure 7D). To evaluate the mechanism through which TLR4/IKKβ modulates ceramide levels, we investigated the effects of LPS and palmitate on the transcripts for several enzymes that drive ceramide synthesis, including SPT (isoforms 1 and 2), several CerS isoforms, and DES1. LPS and palmitate induced a number of different ceramide biosynthetic enzymes, most notably STP2 and CerS1, -2, and -6 (Figure 7E). In cells expressing the IKK-KD, which failed to accrue ceramide, levels of these transcripts were markedly reduced, and LPS and palmitate failed to alter their expression.

To test the relevance and specificity of IKKβ as a modulator of sphingolipid synthesis in vivo, we treated 22-week-old diet-induced obese mice with the IKKβ inhibitor sodium salicylate (NS). NS had no effect on body weight (Figure 7A) but markedly improved glucose and insulin tolerance (Figure 8, B and C). High-fat feeding increased ceramide levels in soleus, liver, and hypothalamus, but NS treatment blocked its accumulation in all 3 locales (Figure 7, D–I). DAG levels, which also increased in response to high-fat feeding, were unaffected by NS treatment in liver and muscle but were reduced in the hypothalamus. This latter finding is consistent with the earlier results in the lipid infusion model, where TLR4 selectively affected ceramides in peripheral tissues but had a more global effect in the hypothalamus.

Discussion

Two prevailing hypotheses have emerged to explain why an expanding fat mass impairs insulin action. Proponents of the lipotoxicity theory suggest that lipid accumulation in non-adipose tissue sites directly impairs insulin action. In contrast, proponents of the inflammation theory suggest that hyperactivity of the immune

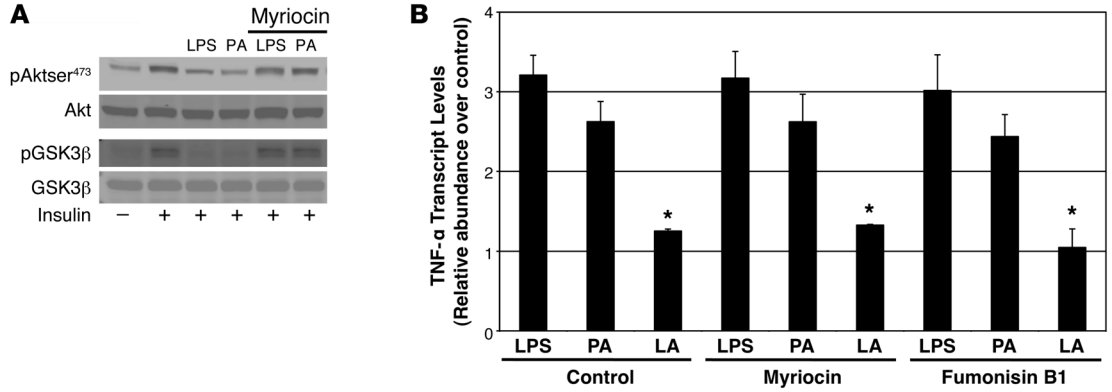

Figure 6

Ceramide is necessary for LPS and PA inhibition on insulin signaling at Akt/PKB in myotubes but not for LPS and PA induction of TNF-α in macrophages. (**A**) C_2C_{12} myotubes were treated with PA (0.75 mM) and LPS (1 μg/ml) for 8 hours in the presence or absence of myriocin (2 μg/ml), followed by 10 minutes of insulin stimulation (100 nM). (**B**) RAW264.7 macrophages were treated with LPS (100 ng/ml) or PA or linoleate (LA) (0.45 mM) in conjunction with either myriocin (10 μM) or fumonisin B1 (50 μM) (**B**). Values are expressed as mean ± SEM (n = 4–5). *P < 0.05 for treatment versus actin control.

system, resulting from lipid activation of TLR4 or from macrophage infiltration of adipose tissue, leads to the overproduction of inflammatory cytokines that perturb metabolic function. The data presented in this study suggest that these 2 pathways are inextricably linked, and that a primary function of inflammatory cytokines is to control the utilization of fatty acids in peripheral tissues. In particular, the results demonstrate that TLR4 alters the metabolic program of skeletal muscle, diverting fatty acids into sphingolipids, which antagonize insulin action. Collectively these data reveal that inflammatory processes are critically linked to metabolic pathways controlling the utilization of excess fat, which has a marked impact on insulin sensitivity.

TLR4, SFAs, and insulin resistance. Several years ago we reported that long-chain SFAs (i.e., palmitate [C16:0], stearate [C18:0], arachidate [C20:0], and lignocerate [C24:0]) induce ceramide synthesis and antagonize insulin signaling in cultured myotubes (29), while unsaturated fatty acids have no effect. Because palmitate is a substrate for SPT (5), which had been deemed to be rate limiting for sphingolipid synthesis, the mechanism by which it influenced ceramide was understandable. However, we were perplexed by the observation that several long-chain SFAs, which were not substrates for SPT, could induce ceramide. The data presented in the current studies provide resolution to this enigma — these are the same fatty acids that augment signaling through TLR4 (15, 30). Thus, SFAs, including palmitate, do not exclusively upregulate ceramide synthesis by fueling the pathway with substrate, but instead by activating the TLR4 cascade to increase rates of de novo ceramide synthesis. These findings have important implications for understanding the regulatory mechanisms controlling production of lipotoxic sphingolipids.

The ability of TLR4 to induce ceramide and insulin resistance occurs, at least in part, via a cell-autonomous mechanism. Evidence supporting this conclusion includes the following: first, LPS antagonizes (via TLR4 and ceramide) insulin-stimulated 2-DOG uptake in muscle strips; second, LPS (via IKKβ and ceramide) antagonizes insulin signaling to Akt/PKB in cultured C_2C_{12} myotubes. These data are consistent with recent findings that TLRs are resident and active in rodent and human muscle cultures (25, 31). Moreover, the findings are consistent with the findings of DiAngelo et al. (32) using *Drosophila*, which indicated that the Toll pathway can impair insulin signaling at the level of Akt/PKB via an evolutionarily conserved, cell-autonomous mechanism.

TLR4 has been shown previously to induce ceramide by rapidly activating sphingomyelinase, which hydrolyzes sphingomyelin into ceramide (33). This enzymatic reaction is an essential and redundant signaling event for a number of receptor systems; ceramides produced in this manner have been shown to cluster different receptors into signaling microdomains, which is requisite for their function (34). However, this increase in ceramide is transient and is unlikely to account for the prolonged elevation in ceramide observed in chronic disease states. Instead, LPS additionally promotes ceramide accumulation by increasing rates of its de novo synthesis. One mechanism through which this occurs is the upregulation of genes associated with ceramide biosynthesis, including different SPT and CerS isoforms (Figure 8). These findings are consistent with prior work revealing that TLR4 ligation induces expression of SPT in a variety of tissues (35–37). The upregulation of biosynthetic genes driving ceramide is dependent upon the IKKβ signaling complex (Figure 9).

Our prior studies reveal that ceramide inhibits glucose uptake by blocking activation of Akt/PKB, and overexpression of a constitutively active form of Akt/PKB protects from ceramide-induced insulin resistance (27). The sphingolipid antagonizes Akt/PKB via at least 2 pathways, culminating on different Akt/PKB domains (38, 39). Some recent attention has been placed on the idea that glucosylceramide, rather than ceramide itself, is the primary antagonist of insulin signaling, as inhibitors of glucosylceramide are potently insulin sensitizing (40, 41). However, glucosylceramides would be predicted to have more dominant actions in adipocytes, as their antagonistic effects are highly dependent upon caveolar domains abundant in that cell type (42). We favor the hypothesis that ceramide, rather than a glucosylated ceramide metabolite, is the key antagonist of insulin action in muscle. Indeed, lipidomic analysis of myotubes revealed that LPS and palmitate induced significant increases in ceramide, but not changes in glucosylceramides or GM3 ganglioside (data not shown). Moreover, GCS inhibitors exacerbated palmitate antagonism of Akt/PKB in myocytes, coinciding with their enhancement of ceramide production (43).

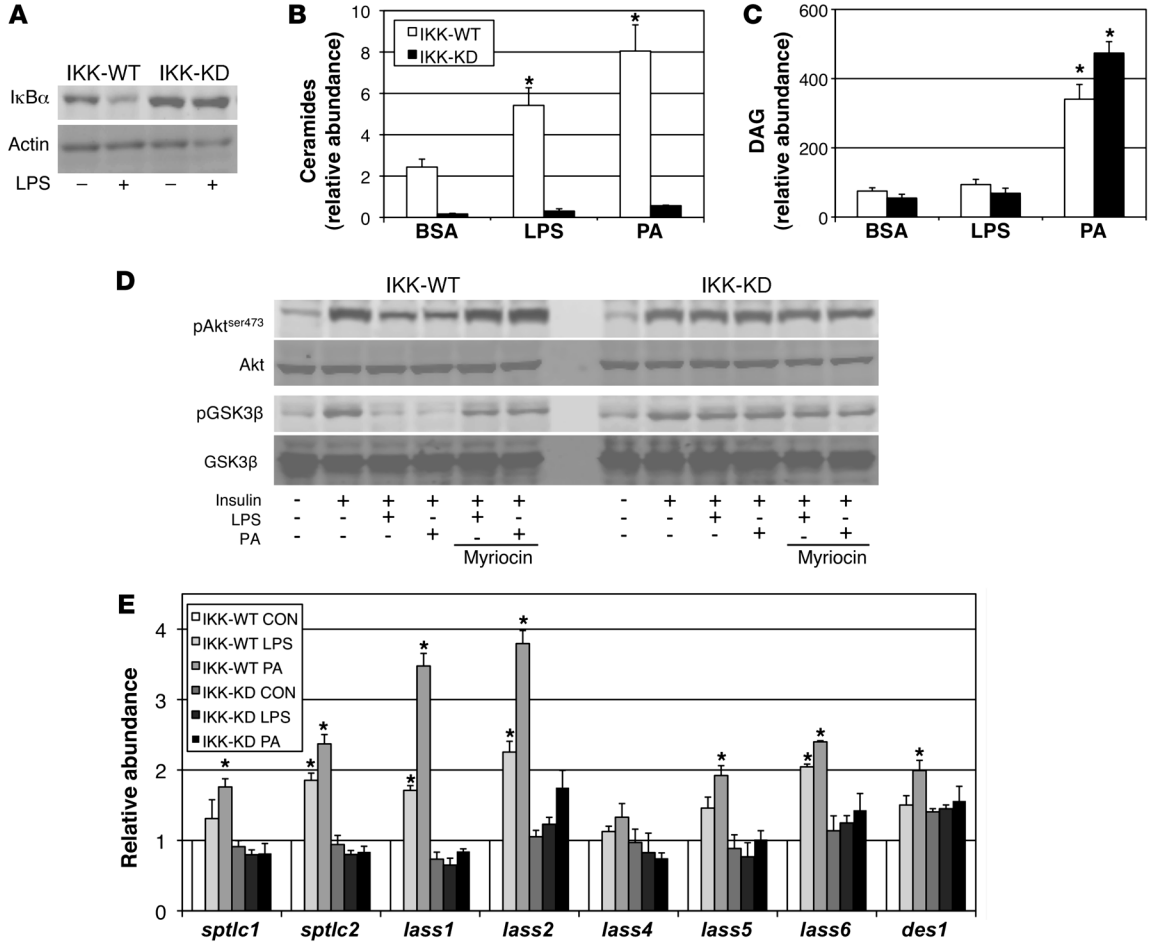

Figure 7

Overexpression of a dominant-negative IKKβ prevents ceramide accrual and LPS- and PA-induced insulin resistance. (**A**) To confirm the lack of IKKβ action in the IKK-KD cells, IκBα levels were measured in WT and KD myotubes following LPS (1 μg/ml) treatment for 1 hour. (**B** and **C**) IKK-KD cells failed to accrue ceramides (**B**), as determined by LC-MS, but did accumulate DAG to relatively normal degrees when treated with LPS (1 μg/ml) or PA (0.75 mM) for 16 hours (**C**). (**D**) IKK-KD cells were resistant to the detrimental effects on Akt/PKB signaling compared with WT cells with PA (0.75 mM) and LPS (1 μg/ml) treatment for 12 hours with or without 1 hour myriocin (10 μM) pretreatment. Murine C_2C_{12} myotubes responded to LPS and PA by selectively upregulating de novo ceramide synthesis in control cells, but not IKK-KD cells. (**E**) Quantitative real-time PCR was performed to determine transcript levels of the enzymes involved in ceramide synthesis on cells treated with LPS (1 μg/ml) and PA (0.75 mM) for 4 hours. *$P < 0.05$ for treatment compared with control. Values are expressed as mean ± SEM (n = 3–5). *$P < 0.05$ for treatment versus BSA control.

The recent surge in interest in the relationships between saturated fats, TLRs, and metabolic homeostasis derives from a high-profile paper by the Flier laboratory (15). Our findings agree with the majority of the conclusions of that study, including the importance of TLR4 in lipid-induced insulin resistance and the highly selective effect of saturated, but not unsaturated, fats on TLR4 action. However, there was a substantive difference related to the experiments involving the infusion of soy-based cocktails. Flier and colleagues found that TLR4 ablation improved insulin sensitivity in animals infused with Intralipid (a commercially available equivalent of our soy oil emulsion), while we only observed an insulin-sensitizing effect in animals infused with the more saturated lard oil. A soy-based emulsion, which is enriched in unsaturated fats, failed to induce an inflammatory response but suppressed insulin sensitivity despite TLR4 ablation in our studies. Intralipid is not completely devoid of saturated fats, however, and we speculate that the inconsistent findings are due to differences in how different strains of animals metabolize the low amounts of saturated fats present in the cocktail. Indeed, while we and others have shown that soy-based infusates fail to induce ceramide (3, 44), Watt et al. reported a substantial induction (45). Moreover, Straczkowski report that Intralipid infusion into people is sufficient to induce ceramide (46).

Hypothalamic insulin and leptin signaling have important roles in body weight regulation as well as in the maintenance of glucose homeostasis (47–50). Fatty acids have been shown previously to impair the signaling cascades and physiologic effects evoked by these hormones via central mechanisms (23, 51). While aberrant accumulation of acyl-CoA and DAG has been implicated as a mediator of FFA-induced impairment of hypothalamic leptin and insulin action (23, 52), this is the first report that ceramide accumulates in the hypothalamus of rodents exposed to high-fat diets or saturated fat–enriched intravenous emulsions. Activation of hypothalamic inflammatory pathways has been implicated in

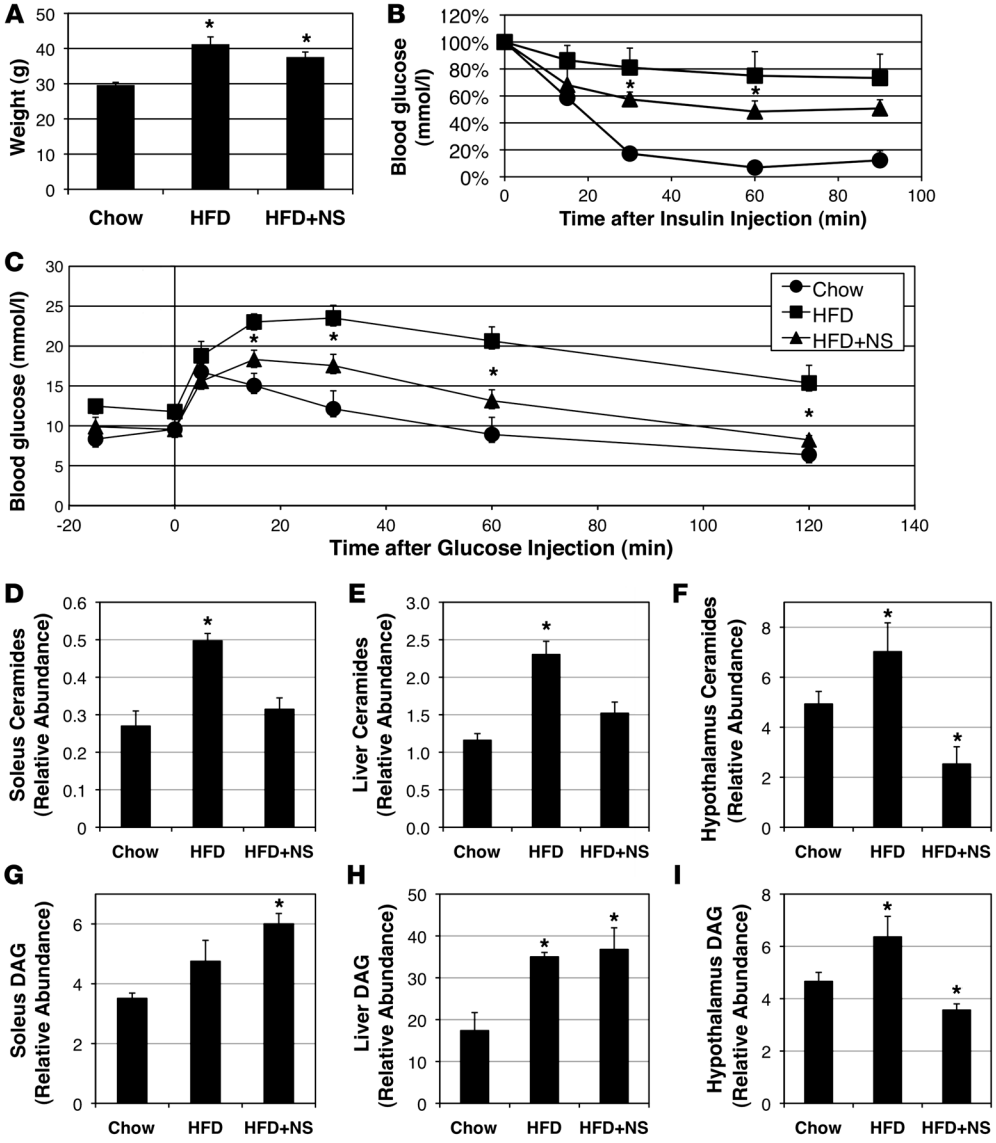

Figure 8
Suppression of IKKβ with NS restores insulin sensitivity via ceramide inhibition. Male C57BL/6 mice were fed either a chow (10% of kcal from fat) or a high-fat diet (HFD; 60% of kcal from fat) from 5 weeks old. At 22 weeks, randomly assigned high-fat diet–fed mice were switched to a high-fat diet supplemented with 6 g/kg NS (HFD+NS) for 6 weeks. (**A**) The high-fat diet was associated with significant weight gain in both groups compared with chow-fed littermates. *$P < 0.05$ for HFD and HFD+NS compared with chow-fed mice. (**B** and **C**) Insulin and glucose tolerance were improved in the high-fat diet plus NS group. *$P < 0.05$ for HFD+NS compared with HFD alone. (**D**–**I**) Addition of NS to the high-fat diet effectively inhibited ceramide accrual in soleus, liver, and hypothalamus (**D**–**F**; *$P < 0.05$ for HFD compared with chow and HFD+NS) but exerted only an inhibitory effect on DAG in hypothalamus (**I**), not soleus or liver (**G** and **H**). Values are expressed as mean ± SEM ($n = 8$). *$P < 0.05$ for HFD compared with chow.

mediating onset of obesity (47), but we did not observe a statistically significant divergence in body weight in high-fat diet–fed animals treated with or without NS, a finding corroborated by others (53). However, it is plausible that such an effect could become apparent with longer treatments.

TLR4, SFAs, and cytokine production. Elimination of TLR4 selectively in hematopoietic-derived cells via bone marrow transplant ameliorates lipid-induced insulin resistance and inflammation in adipose and liver (14). Thus, TLR4 appears to additionally modulate insulin sensitivity via non-autonomous mechanisms. These findings are also consistent with the aforementioned studies using *Drosophila*, which identified non-autonomous (as well as cell autonomous) mechanisms by which TLRs influence insulin signaling (32). Many of the cytokines induced by TLR4 (e.g., TNF-α) in turn promote de novo ceramide synthesis. Thus, we predict that ceramide is a common molecular intermediate linking numerous inflammatory mediators to the antagonism of insulin action. The existence of such a broad scope of factors that induce insulin resistance and induce sphingolipid synthesis reinforces the idea that ceramide lies at the nexus of numerous signaling networks that modulate insulin action and helps explain the remarkable efficacy of ceramide-lowering agents as insulin sensitizers.

The data presented herein confirm numerous reports in the literature that SFAs, but not unsaturated fatty acids, stimulate cytokine secretion from macrophages (11–13, 54). Infusion of lard oil, but not soy oil, in both rats and mice led to a marked inflammatory response and high circulating levels of TNF-α and IL-6 (Figure 2). Unlike the effects in skeletal muscle, this aspect of SFA and TLR4 action appears to be ceramide independent, as myriocin failed to reduce cytokine production in vivo (during lipid infusion) or in cultured macrophages (treated with LPS or palmitate). This conclusion contrasts that of Schwartz et al. (55), who reported that palmitate induction of IL-6 and IL-8 production was dependent upon ceramide. However, we note that in that study myriocin and fumonisin only modestly impaired cytokine expression, and a substantial induction was observed in the absence of ceramide. Moreover, the experimental protocol involved prolonged incubations with

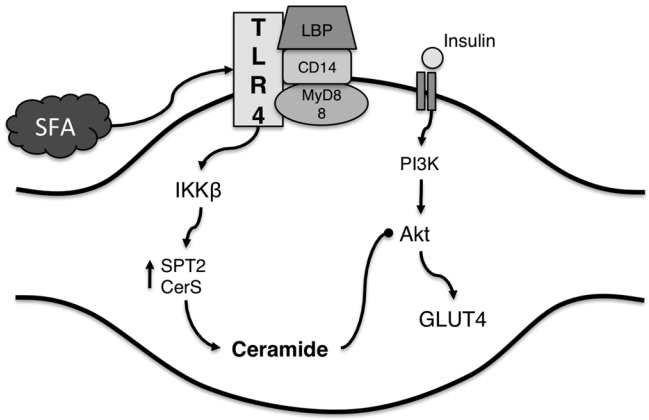

Figure 9
Diagram of possible events involved in TLR4 action on ceramides.

the ceramide synthesis inhibitors, which could affect the sphingomyelin pool needed to initiate TLR4 signaling. Other studies have supported the hypothesis that ceramide does not induce cytokine synthesis (56).

The mechanism through which SFAs may enhance TLR4 signaling has been controversial and elusive. The fatty acid component of LPS is sufficient to activate TLR4, and many groups have reported that SFAs, but not unsaturated fatty acids, are TLR4 agonists (11–15). However, Erridge and Samani (57) found that SFA solutions of varying fatty acid chain length failed to activate TLR4 in HEK-293 kidney and RAW264.7 macrophage cell cultures, implicating BSA contaminated with LPS as the relevant agonist. Indeed, Schwartz and colleagues (55) observed a synergistically amplified inflammatory response in cells exposed to SFA and LPS together as compared with LPS or SFA alone. Thus, one possible explanation for the selective effects of SFAs on TLR4 signaling is that it enhances effects of contaminating LPS. Alternatively, Wong et al. (58) suggested that SFAs induced TLR4 dimerization by facilitating its recruitment into lipid rafts, which preferentially derive from lipids with saturated acyl chains.

Summary. Recent studies in 2 different patient populations have revealed strong correlations among plasma ceramides, circulating cytokines, and insulin resistance (59–61). However, the relative order of events was unknown, as inflammatory factors have been shown to stimulate ceramide production, while ceramides have also been reported to induce inflammation. The data presented herein provide directionality for the events, determining that inflammation (e.g., TLR4) lies upstream of ceramide production and is in fact requisite for de novo ceramide synthesis in skeletal muscle. Impressively, rates of ceramide production were independent of circulating lipid levels but were critically dependent upon regulatory events controlled by TLR4. More importantly, the ceramide produced proved to be essential for inflammation-induced insulin resistance, both in vitro and in vivo.

DiAngelo et al. (32) proposed that TLR4 inhibition of Akt/PKB is a conserved response by which cells prepare to combat invading organisms by blocking anabolic pathways promoting nutrient storage and cellular growth. We propose that this TLR4 effect on lipid metabolism involves the diversion of fatty acids away from oxidative pathways (Figure 3 and ref. 31) and into sphingolipids involved in the general eukaryotic stress response (62). One consequence of this event is a reduction in the rate of anabolic processes. While this mechanism likely occurs in a broad number of cell types and conditions, in muscle it manifests itself as an inhibition of glucose transport, protein synthesis, and cell growth.

Collectively, the data reveal a common mechanism through which hyperlipidemia and inflammation converge to induce insulin resistance, placing ceramides at the nexus of these ectopic factors associated with metabolic disease. Future studies delineating how TLR4 and IKKβ control rates of ceramide production could lead to the identification of new regulatory factors and therapeutic targets for combating health complications associated with obesity.

Methods

Animals. Male Sprague-Dawley rats were obtained from Charles River Laboratories. Control (B6129SF1, BALB/c, and C57BL/6) and mutant mice with disruption of TLR4 (C.C3-*Tlr4lps-d*) and TLR2 (B6.129S1-Tlr2tm1Dgen), TNF receptor–null mice, and diet-induced obese and control-fed 26-week-old mice were from The Jackson Laboratory. *Des1*$^{-/+}$ mice were provided by Lexicon Pharmaceuticals Inc., and Mlk3-knockout mice were a gift from Roger Davis (University of Massachusetts Medical School, Worcester, Massachusetts, USA). Studies were conducted in accordance with the principles and procedures outlined in the National Institutes of Health Guide for the Care and Use of Laboratory Animals and were approved by the IACUCs at the University of Utah, Duke University, University of Texas Southwestern Medical Center, and the Duke-National University of Singapore Graduate Medical School.

Animal surgery. For lipid infusion and hyperinsulinemic-euglycemic clamp protocols, rats were anesthetized with ketamine (65 mg/kg) and xylazine (10 mg/kg), and polyethylene catheters were aseptically placed in the left carotid artery (advanced to the aortic arch) or the right jugular vein. Catheters were filled with 3% heparinized saline to maintain patency and exteriorized in the intrascapular region. Buprenorphine (0.03 mg/kg, s.c.) was postsurgically administered for pain control, and animals were allowed to recover (5–7 days) to preoperative weight prior to experiments.

For lipid infusion and hyperinsulinemic-euglycemic clamp protocols, mice were anesthetized with ketamine (100 mg/kg) and xylazine (10 mg/kg), and silicone catheters were aseptically placed in the right jugular vein. Catheters were filled with glycerol (75%) and heparinized saline (250 mU/ml) to maintain patency and exteriorized in the intrascapular region. Buprenorphine (0.03 mg/kg, s.c.) was post-surgically administered for pain control, and animals were allowed to recover (4 days) to preoperative weight prior to experiments.

Hyperinsulinemic-euglycemic clamps. Clamps were performed in conscious, unrestrained animals using swivels and tethers (Instech) to allow uninterrupted movement of the animals without disruption of infusion lines. Hyperinsulinemia was initiated by intravenous infusion of insulin (rats: 10 mU/kg/min; mice: 20 mU/kg/min). Rat blood was sampled from arterial lines at 7-minute intervals and analyzed with a Beckman Glucose Analyzer II (Beckman Coulter). Euglycemia was maintained by variable infusion of 20% dextrose. Mouse whole blood glucose was assayed by glucometer (Bayer Elite), and euglycemia was maintained by variable infusion of 50% dextrose. Steady state was achieved approximately 90 minutes after initiating hyperinsulinemia and maintained for at least 45 minutes. Glucose infusion rates were calculated as the average glucose infusion rate during the steady-state period. Additional blood samples were taken before initiating hyperinsulinemia and at the end of the clamp for analysis of insulin and free fatty acids. For analysis of glucose kinetics in mice, ^{3}H-glucose kinetics were analyzed before and after insulin (4 mU/kg/min) as previously described (3).

Lipid infusion. Glycerol, 20% lard oil, or 20% soy oil emulsions were prepared as previously described (20) and infused at a constant rate of 5 ml/kg/h. To activate lipoprotein lipase, heparin (6 U/h) was added to the triglyceride emulsions. Lipids were infused in animals treated with control injections (normal saline), cylcoserine (25 mg/kg, i.p.), or myriocin (100 mg/kg, i.p.). Drugs were given 12 hours prior to lipid infusion, and equivalent doses were given intravenously at the time of infusion. To prevent occlusion of intravenous lines in mice being infused with glycerol, heparin (0.3 U/h) was included in glycerol-infused mice. Drugs were given 12 hours prior to lipid infusion, and equivalent doses were given intravenously at the time of infusion. Hyperinsulinemic-euglycemic clamps were initiated after 4.5 hours of lipid infusion by intravenous co-infusion of insulin for the duration of the procedure. Following lipid infusion, animals were deeply anesthetized, and soleus muscles and liver were rapidly dissected out and frozen in liquid nitrogen.

Isolated muscles. Palmitate or linoleate was first dissolved in ethanol (200 mM), and ethanol or free fatty acids were conjugated to BSA by diluting 1:25 in Krebs-Henseleit buffer (KHB) supplemented with 20% BSA and heating (55°C for 30 minutes, with occasional vortexing). The final incubation medium was prepared by diluting the conjugated BSA solution 1:8 in freshly oxygenated KHB. Male Sprague-Dawley rats (150–200 grams) were deeply anesthetized with sodium pentobarbital (110 mg/kg, i.p.), and soleus muscles were isolated, laterally bisected, and transferred to 25 ml Erlenmeyer flasks containing 2 ml of KHB supplemented with 2.5% BSA, 8 mM glucose, and 1 mM HEPES (pH 7.2). Muscles were maintained in a shaking water bath at 29°C while being continuously gassed with 95% O_2/5% CO_2. Following this incubation, muscles were rapidly frozen in liquid nitrogen or stimulated with insulin (300 μU) for 60 minutes, and the incorporation of [^{3}H]2-DOG was assessed during the final 20 minutes of the incubation using methods described previously (63). Free fatty acids were present throughout the 2-DOG uptake assay.

Glucose and insulin tolerance tests. Male C57BL/6 mice were fed a normal chow diet or a high-fat diet (D12492; Research Diets, Inc.) from 5 to 22 weeks, at which point half of the high-fat diet–fed mice began receiving high-fat diet with 0.6% NS (D10062205) for 6 weeks. Following this, mice underwent i.p. glucose (G7021; Sigma-Aldrich) and insulin (Actrapid; Novo Nordisk) tolerance tests. For both tests, mice were fasted for 6 hours and received an injection of either glucose (1 g/kg body weight) or insulin (0.75 U/kg body weight). Blood glucose was determined at the times indicated in the figures, using the Bayer Contour glucose meter.

Cell culture. Cells were maintained in DMEM plus 10% fetal bovine serum (Invitrogen). For differentiation into myotubes, C_2C_{12} myoblasts were grown to confluency and the medium was replaced with DMEM plus 10% horse serum (Invitrogen). Myotubes were used for experiments on day 4 of differentiation. For fatty acid treatment, palmitic acid (Sigma-Aldrich; catalog no. P5585) or linoleic acid (Sigma-Aldrich; catalog no. L1012) was dissolved in ethanol and diluted to desired concentration in DMEM containing 2% (wt/vol) BSA (Sigma-Aldrich; catalog no. A9576). BSA was tested (Pyrogent Plus; Lonza) and found to contain trace levels of endotoxin, but by itself was insufficient to activate JNK or induce cytokine synthesis. LPS (catalog no. L8274), myriocin (M1177), and fumonisin B1 (catalog no. 32936) were purchased from Sigma-Aldrich.

Generation of retroviral vectors for stable expression. A derivative of pTS13.1 was generated to make a retroviral HA epitope tagging vector. pTS13.1-HA was made by annealing primer 1 (CTCGAGCGGCCGCGTAATCCGGAACATCGTATGGGTACATGGTGGCGGCGTCGACGTTAACGGTACCC) and primer 2 (GGGTACCGTTAACGTCGACGCCGCCACCATGTACCCATACGATGTTCCGGATTACGCGGCCGCTCGAG) and inserting them into SalI and ClaI sites of pTS13.1. A derivative of the pLPNPX1 vector (64) was generated for hygromycin selection. The pLPNPX1-hygro vector was made by removing the *neo* gene fragment (Bsp119I- BseJI) of pLPNPX1 and replacing it with the *hph* gene from the retroviral vector pTS13.1.

Generation of stable IKK-WT and mutant C_2C_{12}. Dominant-negate IKKβ (IKK-KD, K44M mutation) (a gift from F. Mercurio, Celgene, San Diego, California, USA) (65) cDNA was amplified by PCR to insert in-frame into pTS13.1-HA to generate N-terminally HA-tagged constructs (2 additional alanines were inserted between the HA tag and IKKβ sequence). The HA-tagged IKKβ sequences were digested out with NotI and ClaI and inserted into pLPNPX1-Hygro vector. We transfected 293T cells with pLPNPX1-Hygro IKKβ constructs in conjunction with vectors containing gag/pol (pCgp) and pVSV-g using the calcium phosphate procedure as previously described (64). After 24 hours, supernatant-containing virus was collected, filtered, and used to infect C_2C_{12} cells. Stably transfected cells were selected for in 10% FBS plus 200 mg/ml hygromycin B.

Lipid analysis. For isolation of lipids, pellets were re-suspended in 900 μl ice-cold chloroform/methanol (1:2) and incubated for 15 minutes on ice, then briefly vortexed. Separation of aqueous and organic phases required addition of 400 μl of ice-cold water and 300 μl of ice-cold chloroform. The organic phase was collected into a fresh vial, and lipids were dried under a gentle nitrogen stream. Lipids were measured using the DAG kinase assay (3) or liquid chromatography/mass spectrometry (LC-MS). For LC-MS, an Agilent HPLC system coupled with an Applied Biosystems Triple Quadrupole/Ion Trap mass spectrometer (3200 Qtrap) was used for quantification of individual phospholipids. Multiple reaction monitoring (MRM) transitions were set up for quantitative analysis of various polar lipids (66, 67). Levels of individual lipids were quantified using spiked internal standards, including dimyristoyl phosphatidylcholine (28:0-PC), phosphatidylethanolamine (28:0-PE), dimyristoyl C^{14}-phosphatidylserine (28:0-PS), dimyristoyl phosphatidylglycerol (28:0-PG), C^{17}-ceramide, C^8-glucosylceramide, C^{12}-sphingomyelin, dimyristoyl phosphatidic acid (28:0-PA), which were obtained from Avanti Polar Lipids (Alabaster). Dioctanoyl phosphatidylinositol (16:0-PI) from Echelon Biosciences Inc. was used for phosphatidylinositol quantification. Neutral lipids were analyzed using a sensitivity HPLC/ESI/MRM method, modified from a previous method (68). TAGs were calculated as relative contents to the spiked d5-TAG 48:0 internal standard (CDN isotopes), while DAGs were quantified using 4ME 16:0 Diether DG (Avanti) as an internal standard. Lipids of interest were compared with cellular phosphate levels to ensure equal and accurate comparison between treatments.

Quantitative real-time PCR. Total RNA was extracted and purified from tissues using TRIzol (Invitrogen) according to the manufacturer's recommendations. cDNA was synthesized from mRNA via reverse-transcriptase PCR using a commercial cDNA synthesis kit with oligo(dT) primers (iScript Select cDNA Synthesis; Bio-Rad). Quantitative real-time PCR was performed with Evagreen Ssofast (Bio-Rad) using a Bio-Rad iCycler system. Primer sequences are listed in Supplemental Table 1. A sample containing no cDNA was used as a non-template control to verify the absence of primer dimers. β-Actin reactions were performed side by side with every sample analyzed. Changes in mRNA level of each gene for each treatment were normalized to that of the β-actin control mRNA according to Pfaffle (69).

Protein analysis. Tissue extracts were resolved by SDS-PAGE, transferred to nitrocellulose, and immunoblotted using methods described previously (43). Protein detection was performed using the Odyssey Infrared Imaging System (Li-Cor) according to the manufacturer's instructions. Primary antibodies were from Cell Signaling and secondary antibodies from Li-Cor.

Statistics. Data are presented as the mean ± SEM. Data were compared using 2-tailed Student's *t* test or 2-way ANOVA with Bonferroni's post hoc analysis (GraphPad Software). Significance was set at $P < 0.05$.

Acknowledgments

This work was supported by grants from the NIH (R01DK081456-01 to S.A. Summers, P01DK088761 to P.E. Scherer and D.J. Clegg, F32-DK083866 and TL1-DK081181 to W.L. Holland); the Singapore Ministry of Education Academic Research Fund (MOE2009-T2-2-016); the National Medical Research Council, Singapore (IRG09may004); and the Duke-National University of Singapore Signature Research Program funded by the Agency for Science, Technology and Research, Singapore, and the Ministry of Health, Singapore.

Received for publication April 16, 2010, and accepted in revised form February 2, 2011.

Address correspondence to: Scott A. Summers, Program in Cardiovascular and Metabolic Diseases, Duke-NUS Graduate Medical School, 8 College Road #8-15, Singapore, 169857. Phone: 65.6516.8793; Fax: 65.6534.8632; E-mail: scott.summers@duke-nus.edu.sg.

1. Holland WL, Knotts TA, Chavez JA, Wang LP, Hoehn KL, Summers SA. Lipid mediators of insulin resistance. *Nutr Rev*. 2007;65(6 pt 2):S39–S46.
2. Savage DB, Petersen KF, Shulman GI. Disordered lipid metabolism and the pathogenesis of insulin resistance. *Physiol Rev*. 2007;87(2):507–520.
3. Holland WL, et al. Inhibition of ceramide synthesis ameliorates glucocorticoid-, saturated-fat-, and obesity-induced insulin resistance. *Cell Metab*. 2007;5(3):167–179.
4. Bikman BT, Zheng D, Reed MA, Hickner RC, Houmard JA, Dohm GL. Lipid-induced insulin resistance is prevented in lean and obese myotubes by AICAR treatment. *Am J Physiol Regul Integr Comp Physiol*. 2010;298(6):R1692–R1699.
5. Park TS, et al. Ceramide is a cardiotoxin in lipotoxic cardiomyopathy. *J Lipid Res*. 2008;49(10):2101–2112.
6. Park TS, Rosebury W, Kindt EK, Kowala MC, Panek RL. Serine palmitoyltransferase inhibitor myriocin induces the regression of atherosclerotic plaques in hyperlipidemic ApoE-deficient mice. *Pharmacol Res*. 2008;58(1):45–51.
7. Hojjati MR, Li Z, Jiang XC. Serine palmitoyl-CoA transferase (SPT) deficiency and sphingolipid levels in mice. *Biochim Biophys Acta*. 2005;1737(1):44–51.
8. Shimabukuro M, Higa M, Zhou YT, Wang MY, Newgard CB, Unger RH. Lipoapoptosis in beta-cells of obese prediabetic fa/fa rats. Role of serine palmitoyltransferase overexpression. *J Biol Chem*. 1998;273(49):32487–32490.
9. Glaros EN, et al. Inhibition of atherosclerosis by the serine palmitoyl transferase inhibitor myriocin is associated with reduced plasma glycosphingolipid concentration. *Biochem Pharmacol*. 2007;73(9):1340–1346.
10. Park TS, et al. Inhibition of sphingomyelin synthesis reduces atherogenesis in apolipoprotein E-knockout mice. *Circulation*. 2004;110(22):3465–3471.
11. Lee JY, et al. Reciprocal modulation of Toll-like receptor-4 signaling pathways involving MyD88 and phosphatidylinositol 3-kinase/AKT by saturated and polyunsaturated fatty acids. *J Biol Chem*. 2003;278(39):37041–37051.
12. Lee JY, Sohn KH, Rhee SH, Hwang D. Saturated fatty acids, but not unsaturated fatty acids, induce the expression of cyclooxygenase-2 mediated through Toll-like receptor 4. *J Biol Chem*. 2001;276(20):16683–16689.
13. Lee JY, et al. Differential modulation of Toll-like receptors by fatty acids: preferential inhibition by n-3 polyunsaturated fatty acids. *J Lipid Res*. 2003;44(3):479–486.
14. Saberi M, et al. Hematopoietic cell-specific deletion of toll-like receptor 4 ameliorates hepatic and adipose tissue insulin resistance in high-fat-fed mice. *Cell Metab*. 2009;10(5):419–429.
15. Shi H, Kokoeva MV, Inouye K, Tzameli I, Yin H, Flier JS. TLR4 links innate immunity and fatty acid-induced insulin resistance. *J Clin Invest*. 2006;116(11):3015–3025.
16. Davis JE, Gabler NK, Walker-Daniels J, Spurlock ME. Tlr-4 deficiency selectively protects against obesity induced by diets high in saturated fat. *Obesity (Silver Spring)*. 2008;16(6):1248–1255.
17. Kim F, et al. Toll-like receptor-4 mediates vascular inflammation and insulin resistance in diet-induced obesity. *Circ Res*. 2007;100(11):1589–1596.
18. Poggi M, et al. C3H/HeJ mice carrying a toll-like receptor 4 mutation are protected against the development of insulin resistance in white adipose tissue in response to a high-fat diet. *Diabetologia*. 2007;50(6):1267–1276.
19. Tsukumo DM, et al. Loss-of-function mutation in Toll-like receptor 4 prevents diet-induced obesity and insulin resistance. *Diabetes*. 2007;56(8):1986–1998.
20. Stein DT, et al. The insulinotropic potency of fatty acids is influenced profoundly by their chain length and degree of saturation. *J Clin Invest*. 1997;100(2):398–403.
21. Kleinridders A, et al. MyD88 signaling in the CNS is required for development of fatty acid-induced leptin resistance and diet-induced obesity. *Cell Metab*. 2009;10(4):249–259.
22. Fukuda M, et al. Monitoring FoxO1 Localization in Chemically Identified Neurons. *J NeuroSci*. 2008;28(50):13640–13648.
23. Benoit SC, et al. Palmitic acid mediates hypothalamic insulin resistance by altering PKC-theta subcellular localization in rodents. *J Clin Invest*. 2009;119(9):2577–2589.
24. Choi SJ, Kim F, Schwartz MW, Wisse BE. Cultured hypothalamic neurons are resistant to inflammation and insulin resistance induced by saturated fatty acids. *Am J Physiol Endocrinol Metab*. 2010;298(6):E1122–E1130.
25. Reyna SM, et al. Elevated toll-like receptor 4 expression and signaling in muscle from insulin-resistant subjects. *Diabetes*. 2008;57(10):2595–2602.
26. Chavez JA, Summers SA. Characterizing the effects of saturated fatty acids on insulin signaling and ceramide and diacylglycerol accumulation in 3T3-L1 adipocytes and C2C12 myotubes. *Arch Biochem Biophys*. 2003;419(2):101–109.
27. Summers SA, Garza LA, Zhou H, Birnbaum MJ. Regulation of insulin-stimulated glucose transporter GLUT4 translocation and Akt kinase activity by ceramide. *Mol Cell Biol*. 1998;18(9):5457–5464.
28. Cai D, et al. Local and systemic insulin resistance resulting from hepatic activation of IKK-beta and NF-kappaB. *Nat Med*. 2005;11(2):183–190.
29. Chavez JA, Summers SA. Characterizing the effects of saturated fatty acids on insulin signaling and ceramide and diacylglycerol accumulation in 3T3-L1 adipocytes and C2C12 myotubes. *Arch Biochem Biophys*. 2003;419(2):101–109.
30. Senn JJ. Toll-like receptor-2 is essential for the development of palmitate-induced insulin resistance in myotubes. *J Biol Chem*. 2006;281(37):26865–26875.
31. Frisard MI, et al. Toll-like receptor 4 modulates skeletal muscle substrate metabolism. *Am J Physiol Endocrinol Metab*. 2010;298(5):E988–E998.
32. DiAngelo JR, Bland ML, Bambina S, Cherry S, Birnbaum MJ. The immune response attenuates growth and nutrient storage in Drosophila by reducing insulin signaling. *Proc Natl Acad Sci U S A*. 2009;106(49):20853–20858.
33. Cuschieri J, Bulger E, Billgrin J, Garcia I, Maier RV. Acid sphingomyelinase is required for lipid Raft TLR4 complex formation. *Surg Infect (Larchmt)*. 2007;8(1):91–106.
34. Bollinger CR, Teichgraber V, Gulbins E. Ceramide-enriched membrane domains. *Biochim Biophys Acta*. 2005;1746(3):284–294.
35. Memon RA, et al. Endotoxin and cytokines increase hepatic sphingolipid biosynthesis and produce lipoproteins enriched in ceramides and sphingomyelin. *Arterioscler Thromb Vasc Biol*. 1998;18(8):1257–1265.
36. Memon RA, Holleran WM, Uchida Y, Moser AH, Grunfeld C, Feingold KR. Regulation of sphingolipid and glycosphingolipid metabolism in extrahepatic tissues by endotoxin. *J Lipid Res*. 2001;42(3):452–459.
37. Sims K, et al. Kdo2-Lipid A, a TLR4-specific agonist, induces de novo sphingolipid biosynthesis in RAW264.7 Macrophages, which is essential for induction of autophagy. *J Biol Chem*. 2010; 285(49):38568–38579.
38. Blouin CM, et al. Plasma membrane subdomain compartmentalization contributes to distinct mechanisms of ceramide action on insulin signaling. *Diabetes*. 2010;59(3):600–610.
39. Stratford S, Hoehn KL, Liu F, Summers SA. Regulation of insulin action by ceramide: dual mechanisms linking ceramide accumulation to the inhibition of Akt/protein kinase B. *J Biol Chem*. 2004;279(35):36608–36615.
40. Aerts JM, et al. Pharmacological inhibition of glucosylceramide synthase enhances insulin sensitivity. *Diabetes*. 2007;56(5):1341–1349.
41. Zhao H, et al. Inhibiting glycosphingolipid synthesis improves glycemic control and insulin sensitivity in animal models of type 2 diabetes. *Diabetes*. 2007;56(5):1210–1218.
42. Kabayama K, et al. Dissociation of the insulin receptor and caveolin-1 complex by ganglioside GM3 in the state of insulin resistance. *Proc Natl Acad Sci U S A*. 2007;104(34):13678–13683.
43. Chavez JA, et al. A role for ceramide, but not diacylglycerol, in the antagonism of insulin signal transduction by saturated fatty acids. *J Biol Chem*. 2003;278(12):10297–10303.
44. Yu C, et al. Mechanism by which fatty acids inhibit insulin activation of insulin receptor substrate-1 (IRS-1)-associated phosphatidylinositol 3-kinase activity in muscle. *J Biol Chem*. 2002;277(52):50230–50236.
45. Watt MJ, Hevener A, Lancaster GI, Febbraio MA. Ciliary neurotrophic factor prevents acute lipid-induced insulin resistance by attenuating ceramide accumulation and phosphorylation of c-Jun N-terminal kinase in peripheral tissues. *Endocrinology*. 2006;147(5):2077–2085.
46. Straczkowski M, et al. Relationship between insulin sensitivity and sphingomyelin signaling pathway in human skeletal muscle. *Diabetes*. 2004; 53(5):1215–1221.
47. Zhang X, Zhang G, Zhang H, Karin M, Bai H, Cai D. Hypothalamic IKKbeta/NF-kappaB and ER stress link overnutrition to energy imbalance and obesity. *Cell*. 2008;135(1):61–73.
48. Gelling RW, et al. Insulin action in the brain con-

tributes to glucose lowering during insulin treatment of diabetes. *Cell Metabolism*. 2006;3(1):67–73.
49. Obici S, Zhang BB, Karkanias G, Rossetti L. Hypothalamic insulin signaling is required for inhibition of glucose production. *Nature Medicine*. 2002;8(12):1376–1382.
50. Myers MG, Munzberg H, Leinninger GM, Leshan RL. The geometry of leptin action in the brain: more complicated than a simple ARC. *Cell Metab*. 2009;9(2):117–123.
51. Posey KA, et al. Hypothalamic proinflammatory lipid accumulation, inflammation, and insulin resistance in rats fed a high-fat diet. *Am J Physiol Endocrinol Metab*. 2009;296(5):E1003–E1012.
52. He W, Lam TKT, Obici S, Rossetti L. Molecular disruption of hypothalamic nutrient sensing induces obesity. *Nat NeuroSci*. 2006;9(2):227–233.
53. Minge CE, Bennett BD, Norman RJ, Robker RL. Peroxisome proliferator-activated receptor-gamma agonist rosiglitazone reverses the adverse effects of diet-induced obesity on oocyte quality. *Endocrinology*. 2008;149(5):2646–2656.
54. Lee JY, et al. Saturated fatty acid activates but polyunsaturated fatty acid inhibits Toll-like receptor 2 dimerized with Toll-like receptor 6 or 1. *J Biol Chem*. 2004;279(17):16971–16979.
55. Schwartz EA, et al. Nutrient modification of the innate immune response: a novel mechanism by which saturated Fatty acids greatly amplify monocyte inflammation. *Arterioscler Thromb Vasc Biol*. 2010;30(4):802–808.
56. Jozefowski S, et al. Ceramide and ceramide 1-phosphate are negative regulators of TNF-alpha production induced by lipopolysaccharide. *J Immunol*. 2010;185(11):6960–6973.
57. Erridge C, Samani NJ. Saturated fatty acids do not directly stimulate Toll-like receptor signaling. *Arterioscler Thromb Vasc Biol*. 2009;29(11):1944–1949.
58. Wong SW, Kwon MJ, Choi AM, Kim HP, Nakahira K, Hwang DH. Fatty acids modulate Toll-like receptor 4 activation through regulation of receptor dimerization and recruitment into lipid rafts in a reactive oxygen species-dependent manner. *J Biol Chem*. 2009;284(40):27384–27392.
59. de Mello VD, et al. Link between plasma ceramides, inflammation and insulin resistance: association with serum IL-6 concentration in patients with coronary heart disease. *Diabetologia*. 2009;52(12):2612–2615.
60. Haus JM, et al. Plasma ceramides are elevated in obese subjects with type 2 diabetes and correlate with the severity of insulin resistance. *Diabetes*. 2009;58(2):337–343.
61. Gill JM, Sattar N. Ceramides: a new player in the inflammation-insulin resistance paradigm? *Diabetologia*. 2009;52(12):2475–2477.
62. Hannun YA, Luberto C. Ceramide in the eukaryotic stress response. *Trends Cell Biol*. 2000;10(2):73–80.
63. Brozinick JT Jr, Birnbaum MJ. Insulin, but not contraction, activates Akt/PKB in isolated rat skeletal muscle. *J Biol Chem*. 1998;273(24):14679–14682.
64. Lawrence JT, Birnbaum MJ. ADP-ribosylation factor 6 delineates separate pathways used by endothelin 1 and insulin for stimulating glucose uptake in 3T3-L1 adipocytes. *Mol Cell Biol*. 2001;21(15):5276–5285.
65. Mercurio F, et al. IKK-1 and IKK-2: cytokine-activated IkappaB kinases essential for NF-kappaB activation. *Science*. 1997;278(5339):860–866.
66. Fei W, et al. Fld1p, a functional homologue of human seipin, regulates the size of lipid droplets in yeast. *J Cell Biol*. 2008;180(3):473–482.
67. Chan R, et al. Retroviruses human immunodeficiency virus and murine leukemia virus are enriched in phosphoinositides. *J Virol*. 2008;82(22):11228–11238.
68. Shui G, et al. Toward one step analysis of cellular dynamic lipidome using liquid chromatography coupled with mass spectrometry: application to saccharomyces cerevisiae and schizosaccharomyces pombe lipidomics. *Mol BioSyst*. 2010;6:1008–1017.
69. Pfaffl MW. A new mathematical model for relative quantification in real-time RT-PCR. *Nucleic Acids Res*. 2001;29(9):e45.